Bulletin of the Geological Society of Malaysia, Volume 77, May 2024, pp. 87 - 96
DOI: https://doi.org/10.7186/bgsm77202409

Characteristics of epithermal gold-base metals prospect in the Anggai block, northern Obi Island, Indonesia

Bambang Nugroho Widi, Muhammad Zain Tuakia*, Noor Cahyo Dwi Aryanto, Wahyu Widodo, Hananto Kurnio, Iwan Setiawan, Bambang Pardiarto, Armin Tampubolon, Kusnawan

Research Center for Geological Resources, National Research and Innovation Agency (BRIN), Jl. Sangkuriang No. 21, Bandung 40135, Indonesia
* Corresponding author email address: muha100@brin.go.id

Abstract: The Obi island, located in the North Moluccas Au-Ag-Cu province, hosts several mineral prospects, one of which is gold-base metals in the Anggai block. Several companies have historically explored the area since the end of the 1900s. The ore bodies are white to smoky and brownish-white, banded, laminated, colloform, crustiform, and massive quartz vein structures or textures, trending north northwest to south southeast. The ore bodies consist of gold and base metals hosted in the Bacan Formation and are enveloped by dominantly argillic alteration and the addition of silicic alteration. In this study, we provide several analyses, namely petrography, measurements using Portable Infrared Mineral Analyser (PIMA), Atomic Absorption Spectrometry (AAS), and fluid inclusion analysis, to understand geological and geochemical characteristics related to formation of gold-base metals in the Anggai block. Under the microscope, gold (i.e., electrum) is freely observed and closely occurs with argentite. While galena, chalcopyrite, sphalerite, covellite, chalcocite, and pyrite are mainly observed together. The correlation coefficient between Au and other metals shows a strong positive correlation with Zn (r = 0.810188) and a weak positive correlation with Ag (r = 0.459857). Ag shows only a weak positive correlation to Au, while the other elements show a strong positive correlation. In addition, Cu, Pb, and Zn show a strong positive correlation with each other. The micro-thermometry analysis of fluid inclusions shows two modes of homogenization temperature (Th) and salinity: 180-200 °C and 240-280 °C, and 1.4-1.6 and 1.9-2.2 wt% NaCl eq., respectively, suggesting overprinting evidence to enrich the ore bodies with occurrences of gold and base metals in the quartz veins. Gold-base metals were probably carried by the sulfide complex, which later precipitated during the cooling of the hydrothermal fluid.

Keywords: Anggai area, Obi Island, gold-base metals, fluid inclusions, cooling of hydrothermal fluid

INTRODUCTION

Western Halmahera, Bacan, and Obi islands host several deposit types: epithermal gold-base metals, porphyry Cu, and possibly skarn, categorized as the North Moluccas Au-Ag-Cu province (van Leeuwen, 2018). This metal province is less prominent than other metal provinces in Indonesia. However, Gosowong, an epithermal Au-Ag deposit, provides an estimated resource of 4.4 million tonnes (Mt) @ 27.9 g/t Au, containing 4 Moz Au (Clark & Gemmell, 2018). In addition, the Obi island hosts several mineral prospects, namely epithermal gold-base metal veining of Ambon-Anggai, secondary copper in breccia in Sesepe, and possibly skarn-associated gold of Obilatu, hosted by upper Eocene-middle Miocene volcanic rocks (Prihatmoko & Nugroho, 1998; Nur *et al*., 2016). Several other porphyry copper-gold occurrences were also found on Bacan Island, one of which is Kaputusan that has a moderate Cu-Au resource (Bering, 1986).

Administratively, the Anggai gold prospect is located in the Anggai village at the northern part of Obi Island, North Maluku Province. The area is accessible by airplane from Jakarta to Ternate and then to Bacan for about 3 hours and 15 minutes, respectively. Then, from Bacan to Obi Island is continued by boat for about 7-8 hours and finally by car to reach the prospect area that takes about 30 minutes. Thousands of miners have mined this area in more than 300 locations (pits), using traditional and semi-automatic methods, which started before 2000 (Local miners, personal communication, August 2007). The artisanal workers are scattered over approximately 300 ha, following a striking corridor of about 200 m wide mineralization zone extending southward. Some more prominent veins appear and continue to follow the strike for several hundred meters.

Several companies and researchers have studied the Anggai area since the end of the 1900s (Prihatmoko & Nugroho, 1998; Nur *et al*., 2016). Starting in 1995, Obi

0126-6187; 2637-109X / Published by the Geological Society of Malaysia.

Minerals, a subsidiary of Broken Hill, drilled ten boreholes with a total depth of 2,648.3 m and the yield indicated geological resources of 6.8 Mt @ 2.35 g/t Au (Prihatmoko & Nugroho, 1998). In 2007, The Center for Geological Resources of Indonesia conducted an inventory of mineral resources. Several samples in Anggai village resulted in up to 5 gr/t Au from stream sediments, 1 gr/t Au from the soil, and 1,803 gr/t Au from rocks (Sudarya & Faisal, 2007). Then, in 2010 and 2011, Ashburton Minerals Ltd., an Australian mining company, performed a 77 km^2 surface exploration program in and around the artisanal gold mining area and concluded that the Anggai is an epithermal Au-Ag vein or breccia-type deposit. In addition, Prihatmoko & Nugroho (1998) and Nur *et al*. (2016) conducted some laboratory analyses on samples from the Anggai area. They concluded that gold-base metals in Anggai formed in temperatures and salinity ranging from 160-300 °C and 2.0-3.5 wt% NaCl eq., respectively, with a pressure of about 23 to 28 bar, within a depth range of 250 to 300 m below paleo-water table. However, the previous studies provide a less detailed explanation of the geochemical characteristics and physicochemical conditions during the formation of gold-base metals in the Anggai block.

This study gathered results from several analytical methods such as petrography, AAS, PIMA, and fluid inclusion micro-thermometry from samples of unaltered and altered host rocks and ore bodies. The results provide an understanding of geological and geochemical characteristics and give more information and discussion related to ore-forming fluid and its physicochemical condition during the precipitation of metals in the Anggai block.

GEOLOGICAL BACKGROUND

Regional geology

The Obi island is arranged in the southernmost of a north-south archipelago of the eastern part of the Molucca Sea. Two significant faults tectonically bound the island: the Sorong-Maluku Fault in the north and the Sorong-North Sula Fault in the south (Hamilton, 1979; Hall *et al*., 1995) (Figure 1). In geological order, Obi Island consists of the Mesozoic ultramafic and metamorphic rocks unconformably overlain by the series of Tertiary interbedded sedimentary-volcano and intrusive rocks and Quaternary sediments (Sudana *et al*., 1994; Prihatmoko & Nugroho, 1998) (Figure 2). The Mesozoic and even older rocks are similarly found in Bacan Island which represents the Australian continental crust within the Sorong fault system (Ali & Hall, 1995; Hall *et al*., 1995). However, the oldest Neogene subduction-related volcanic rocks on Obi Island are older than those on Bacan Island (Baker & Malaihollo, 1996). This condition is related to the tectonic activity of Molucca Sea, which began to subduct toward Halmahera Island in 17-15 Ma, producing volcanic rocks in Obi Island at age ~11 Ma (Baker & Malaihollo, 1996; Malaihollo & Hall, 1996). Prihatmoko & Nugroho (1998) suggested that the oldest volcanic rock (Oligocene-early Miocene Bacan Formation) in Obi Island, which hosted the Anggai gold-base metals prospect, is an arc-related tectonic (post-collisional) similar to the Moon arc in the Vogelkop, Irian Jaya. This oldest volcanic rock tended to drift along with the Mesozoic rocks since the middle Miocene when the Sorong fault was actively driving west (Dow & Sukamto, 1984; Prihatmoko & Nugroho, 1998). In addition, the complex formation of Obi Island represents occurrences of faults, folds, and lineaments in this area (Sudana *et al*., 1994) (Figure 2). Those structures show mainly similar directions, namely west-east, northwest-southeast, northeast-southwest, and north-south (Sudana *et al*., 1994) (Figure 2).

Local geology

The rock units scattered in the Anggai area are mainly volcanic rocks of the Bacan Formation consisting of lava,

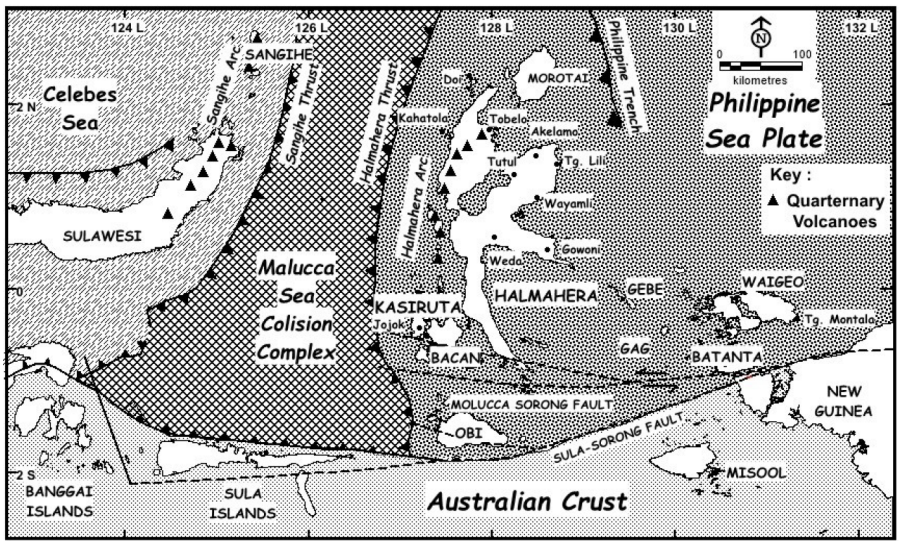

Figure 1: Tectonic setting map of Halmahera and surrounding islands showing Obi Island is bordered by Sorong faults in the northern and southern part of the island (Hall *et al*., 1995).

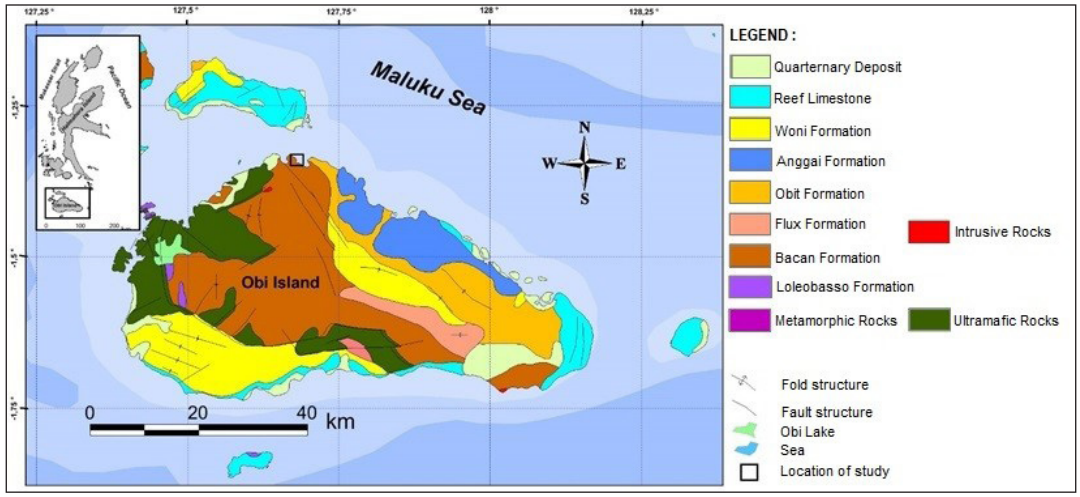

Figure 2: Geological map of Obi Island showing Mesozoic ultramafic-metamorphic rocks and Tertiary volcanic, sedimentary, and intrusive rocks covered by Quaternary sediments (Modified from Sudana *et al*., 1994).

volcanic breccias, tuff, and sedimentary rocks (Sudana *et al*., 1994; Prihatmoko & Nugroho, 1998) (Figures 2, 3a-b). The lava shows a porphyritic texture with a light grey to grey color consisting of plagioclase and pyroxene minerals (Figure 3a). Under the microscope, plagioclase exhibits a subhedral to anhedral shape, polysynthetic twinning and partially altered to carbonate, sericite, chlorite, and clay minerals (Figures 3c-e). Pyroxenes exhibit a greenish-pale color, fine to medium grain (ca.3 mm), anhedral to subhedral shape, micro-cracks that are filled by carbonate minerals and chlorite, and a small number of opaque minerals (Figures 3c-e). In addition, carbonate veinlets were observed cutting into the rocks.

Volcanic breccias were found as part of lava consisting of andesite fragments with subangular to angular shapes and grey to dark grey color (Figures 3b & c). This breccia was well observed in the Anggai River (Figure 3b). Tuff is widely spread in the Anggai area, mainly in the southern part. Tuff is relatively youngest, which overlies lava and volcanic breccia. Tuff comprises fine-grained volcanic materials with a brown to reddish-brown color.

In the Anggai block, the mineralization corridor follows the fractured zone (Figures 2 & 4). It is proven by the orientation of quartz veins that are mostly striking north northwest-south southeast, similar to the fractured zone (Figure 3). It means that the fractured zone acted as the pathway to channel up the hydrothermal fluid to form mineralization in the Anggai area.

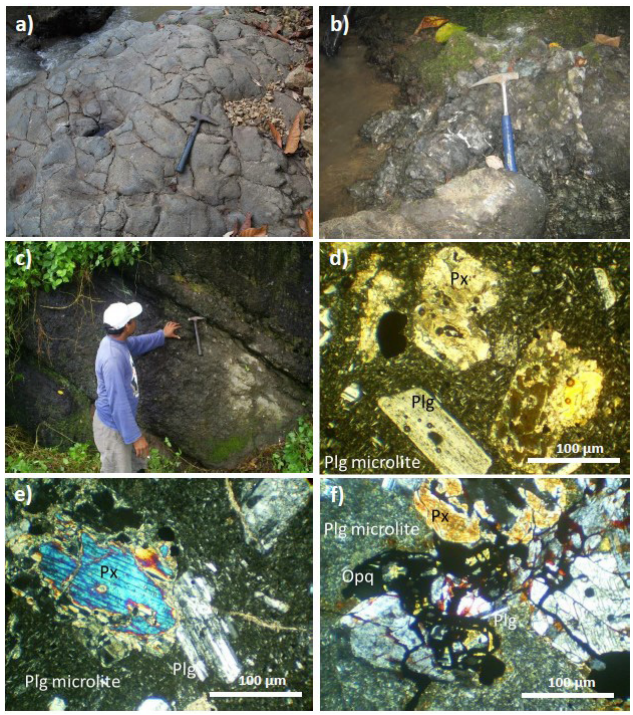

Figure 3: Outcrop photographs of lava at A-003R (a) and volcanic breccia at A-004 exposed in the Anggai River (b) and (c). d-f) Photomicrographs of unaltered host rocks of pyroxene andesite in the Anggai area. Abbreviation: Px=pyroxene; Plg=plagioclase; and Opq=opaque minerals.

SAMPLING AND ANALYTICAL METHODS

Fieldwork was emphasized on mapping the local geology, hydrothermal alteration, and ore bodies. A number of representative samples for the Anggai block were collected, including quartz veins and unaltered and altered host rocks (Figure 4). A total of 14 samples were sent to the Center for Geological Resources (PSDG), Bandung, Indonesia to conduct geochemical analysis for Au, Ag, Cu, Pb, and Zn elements. Those samples were prepared using aqua regia technique, then measured by Atomic Absorption Spectrometry (AAS). The detection limit for Au is about 1 ppb, and other elements such as Cu, Pb, Zn, and Ag were about 2, 4, 2, and 1 ppm, respectively. About 18 samples were prepared for petrographic analysis and were observed

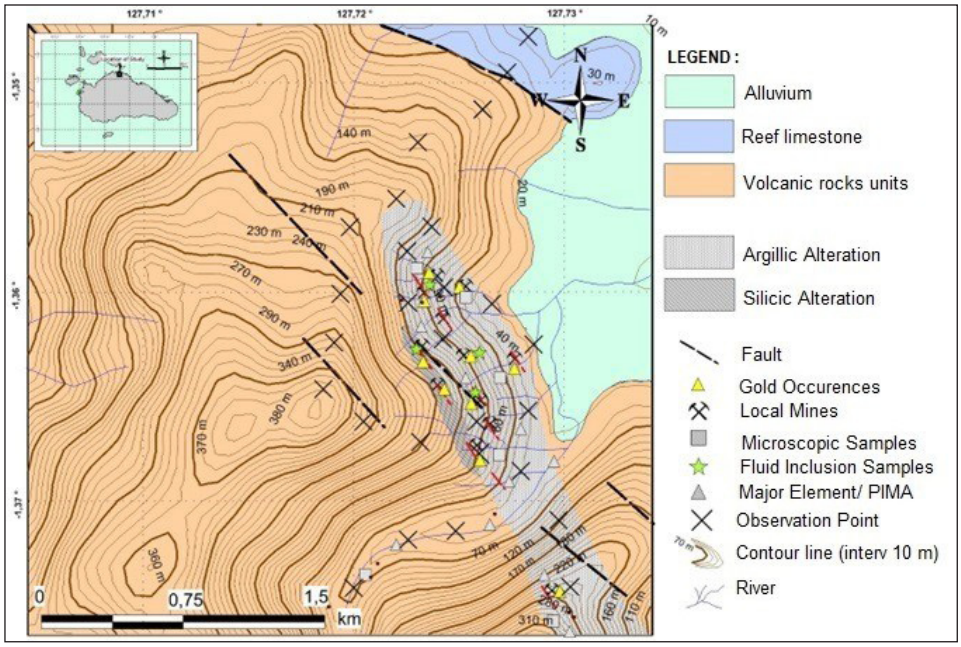

Figure 4: Geological map of the Anggai block showing north-northwest to south-southeast trending mineralized zones and sample locations.

under a Nikon polarizing microscope at the Center for Geological Resources (PSDG), Bandung, Indonesia. Clay minerals were analyzed using Portable Infrared Mineral Analyser (PIMA) of Integrated Spectronics Pty Ltd. on 22 selected samples, conducted in-situ in the field to investigate the hydrothermal mineral assemblages. Each sample was measured in at least three different areas for approximately 5 seconds. About 4 samples were sent to the former Research Center for Geothecnology of Indonesian Institute of Sciences (LIPI) for fluid inclusion analysis, conducted using a Nikon optic microscope equipped with a LINKAM THMS 600 heating–freezing stage to determine homogenization and ice-melting temperatures. Salinities were calculated from the final ice-melting temperatures (Roedder, 1984) and expressed as wt% NaCl equivalent.

RESULTS

Ore characteristics

The mineralized zone in the Anggai block is estimated to be more than 2 km long and 200 m wide, striking north-northwest to south-southeast. The ore bodies are found in many local mining pits with depths up to 50 m below sea level with an average depth of 5-30 m hosted by volcanic rocks (i.e., lava, volcanic breccia, and tuff). The thickness of ore bodies in Anggai is about a few centimeters up to 60 cm, showing white to smoky and brownish-white color, banded, laminated, colloform, crustiform, and having massive quartz vein structures or textures which consist of gold and base metals (Figures 5a-e). Gold is easily found in specific locations within quartz veins as visible gold eg., on Santari Hill (Figure 5d). The visible gold exhibits a sharp to semi-

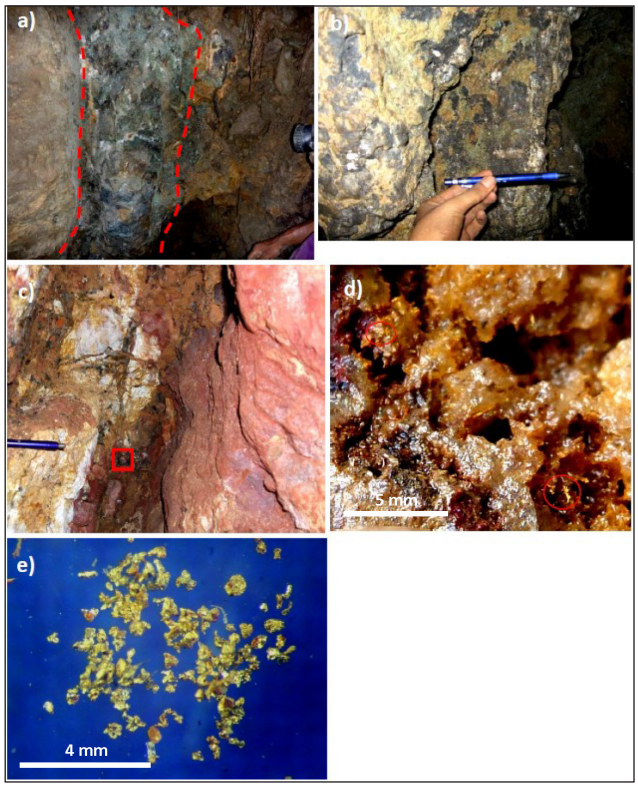

Figure 5: Gold-base metals bearing quartz veins in the artisanal mining pits of Anggai block with a thickness of about 0.3-2 m (a-d) and panned gold grains from the veins (e).

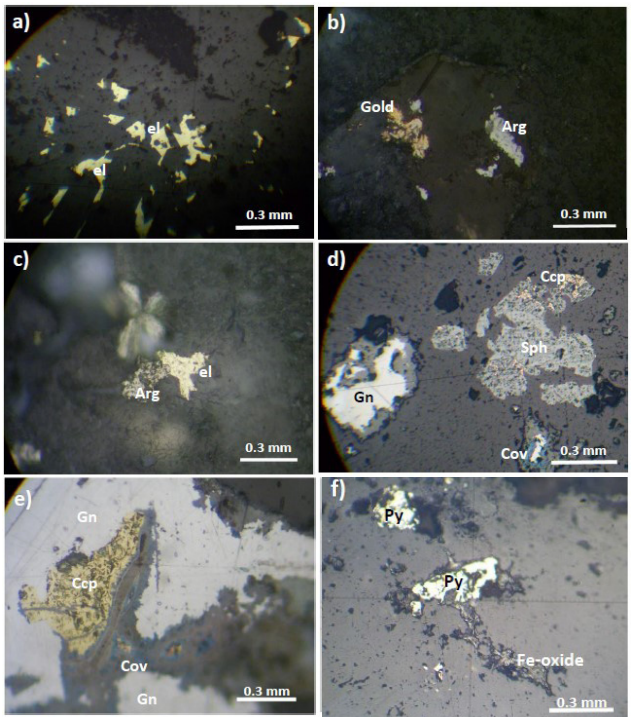

Figure 6: Photomicrographs of quartz vein samples from Anggai ore bodies under cross Nicol that show the occurrences of gold (electrum) (a) and associated with argentite (b-c); base metals in the form of galena, chalcopyrite, covellite/chalcocite and sphalerite (d-e); and pyrite with Fe-oxide (f). Abbreviation: el=electrum; Arg=argentite; Cpy=chalcopyrite; Cov=covelite; Gn=galena; Py=pyrite; Cct=chalcocite; and Sph=sphalerite.

Figure 7: a-d) Outcrop photograph and photomicrographs of hydrothermal breccia in the Anggai block showing altered lithic fragments of pyroxene andesite setting in the quartz±chlorite cement; e) Outcrop photograph of argillic alteration dominated by clay minerals exposed well at Anggai River, and f) silicified lava at Anggai Hill. Abbreviation: Qtz=quartz; Chl=chlorite; and LF=lithic fragments.

angular shape and needle-like structure in the cavity of the quartz veins and the panned grains (Figures 5d-e). The most common base metal minerals observed during fieldwork and microscopic analysis are chalcopyrite, galena, and sphalerite (Figure 5b). Gold (i.e., electrum) is easily observed and associated with argentite under the microscope (Figures 6a-c). Galena, chalcopyrite, and sphalerite were mostly observed together with pyrite (Figure 6d & e). In addition, covellite and chalcocite were also observed at the edge of chalcopyrite during the supergene processes (Figures 6d & e). Fe-oxide was also observed microscopically replacing pyrite as the supergene product (Figure 6f).

Hydrothermal breccia is also exposed to form a vein zone showing a collective of small veinlets. The appearance of the hydrothermal breccia vein is shown in Figure 7a. Microscopically, hydrothermal breccia shows altered lithic fragments of pyroxene andesite setting in the quartz±chlorite cement (Figures 7b-c). The occurrences of alteration zones also identifies the hydrothermal activities in Anggai (Figures 7b-f). The alterations were mainly observed in the volcanic rocks of the Bacan Formation, which are mainly argillic with the addition of silicic in specific areas (Figures 4, 7e & f). The argillic alteration is dominated by clay minerals (montmorillonite and kaolinite), with minor amounts of halloysite, alunite, and paragonite (Figure 7e). In contrast, the silicic alteration consists mainly of silica minerals with minor sericite (Figures 4 and 7f). Another alteration in the area in Anggai is propylitic, which occurred in a limited area and was not mappable. The propylitic alteration consists of dominantly Fe-chlorite, epidote, and carbonate minerals with a minor dickite and gypsum. In addition, illite/muscovite and small amounts of nontronite and phengite were also observed in the very limited area.

Ore chemistry

The 14 quartz vein samples taken from artisanal pits were analyzed using AAS to obtain concentrations of Au, Ag, Cu, Pb, and Zn (Table 1). The results yielded Au concentrations ranging from 0.833 to 509.634 ppm (with an average of 58.743 ppm), Ag concentrations ranging from 2 to 174 ppm, Cu concentrations ranging from 0.01 to 0.91 wt%, Pb concentrations ranging from 0.14 to 40.93 wt%, and Zn concentrations ranging from 0.19 to 11.48 wt% (Table 1). Those elements' correlation coefficients (r) were calculated and summarized in Table 2. Au shows a strong positive correlation with Zn (r = 0.810188) and a weak positive correlation with Ag (r = 0.459857) (Table 2). Ag shows only a weak positive correlation with Au, while with other elements are strongly positively correlated (Table 2). Zn shows a strong positive correlation with Au,

Table 1: AAS analysis results of the quartz vein in the Anggai block.

No.	Sample code	Au (ppm)	Ag (ppm)	Cu (wt%)	Pb (wt%)	Zn (wt%)
1	AH-1	39.448	11	0.16	0.38	0.42
2	AH-2	12.703	15	0.37	0.47	0.6
3	AH-5	30.646	174	0.91	40.93	8.13
4	AH-6	18.388	8	0.06	0.74	0.36
5	AH-7	29.145	3	0.05	0.41	0.33
6	AH-8	49.940	4	0.28	3.48	1.14
7	AH-10	30.283	5	0.06	0.35	0.32
8	AH-11	37.817	3	0.06	0.47	0.28
9	AH-12	20.698	6	0.15	0.16	0.19
10	AH-16	10.474	8	0.01	0.45	0.28
11	AH-17	509.634	103	0.28	0.45	11.48
12	AH-19	4.626	10	0.17	1.18	1.44
13	AH-20	27.772	6	0.12	1.49	0.53
14	A -36	0.833	2	0.02	0.14	0.21

Table 2: Correlation coefficients of Au and other elements in the Anggai block.

	Au (ppm)	Ag (ppm)	Cu %	Pb %	Zn %
Au (ppm)	1				
Ag (ppm)	0.459857	1			
Cu %	0.149772	0.861884	1		
Pb %	-0.05498	0.848367	0.892593	1	
Zn %	0.810188	0.884246	0.646191	0.525738	1

Ag, Cu, and Pb elements with r values of more than 0.5 (Table 2). In addition, Cu, Pb, and Zn are strongly positively correlated (Table 2).

Ore-fluid characteristics

Fluid inclusion analysis was performed on four randomly selected samples of quartz veins taken from artisanal pits. Under the microscope, the quartz crystals exhibit two generations. The first generation is a relatively older, blur, mosaic, medium to coarse grain size, granular to prismatic in anhedral to subhedral shapes, and commonly related to alteration minerals and underwent decrepitated. The second generation is relatively younger, showing transparent, granular, prismatic, crustiform, and drussy textures, mosaic, and commonly occurring as veinlets with more small inclusion. At room temperature, the fluid inclusions are single- and two-phase liquid-rich with minor single-phase vapor inclusions ranging from <1 to 34 μm. Those inclusions have negative crystal, irregular, rounded, elongated, and frequently necking down forms (Figure 8). However, measurement was only conducted in the fluid inclusions that are more than 2.5 μm in size, considered primary in origin.

The homogenization temperatures (Th) of fluid inclusions in the quartz veins range from 185 to 300 °C (Figure 9a). The final ice-melting temperatures of fluid inclusions range from −1.2 to −0.8 °C. The salinity of fluid inclusions ranges from 1.4 to 2.1 wt % (average 1.8 wt%) NaCl equivalent (Figure 9b). The calculated density of fluid inclusions ranging from 0.702 to 0.886 g cm^{-3} inversely with decreasing the temperature.

DISCUSSION

The Anggai gold-base metals prospect is hosted by the Oligocene-early Miocene Bacan Formation, consisting of andesite lavas, volcanic breccia, and tuff. These oldest volcanic rocks resulted from older magmatism activity unrelated to the eastward Molucca Sea plate subduction, which was initiated in 17-15 Ma (Baker & Malaihollo, 1996; Malaihollo & Hall, 1996). On the other hand, these volcanic rocks indicate an arc-related tectonic (post-collisional) typical of the Irian Bird Head volcanic rocks (Prihatmoko & Nugroho, 1998). Biotite phenocrysts of hornblende-biotite andesite in the Sesepe area revealed 39.8 ± 0.8 Ma (late Eocene) (Prihatmoko & Nugroho, 1998). The

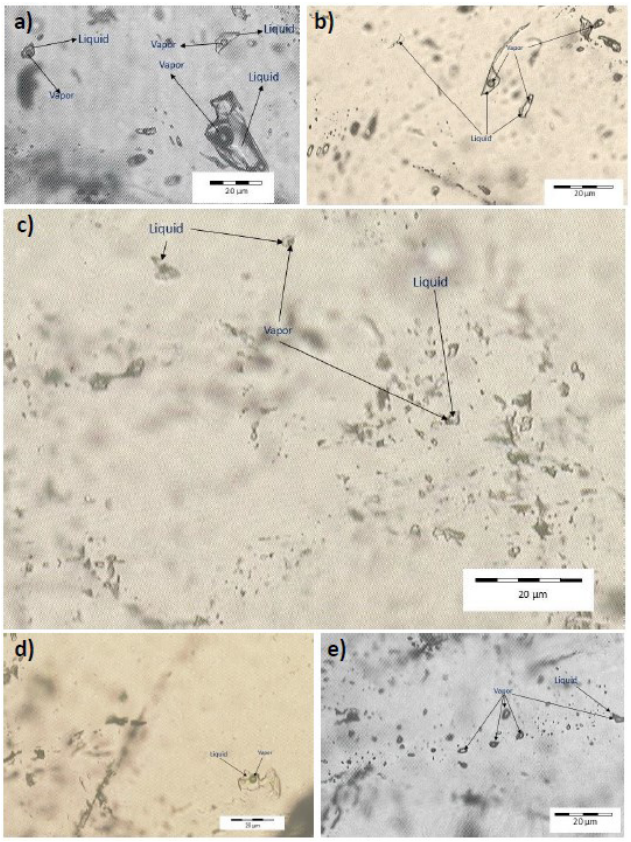

Figure 8: a-e) Photomicrographs of representative fluid inclusions in the Anggai block exhibiting single liquid- and vapor-rich inclusions and two-phase liquid-rich inclusions with various sizes and shapes.

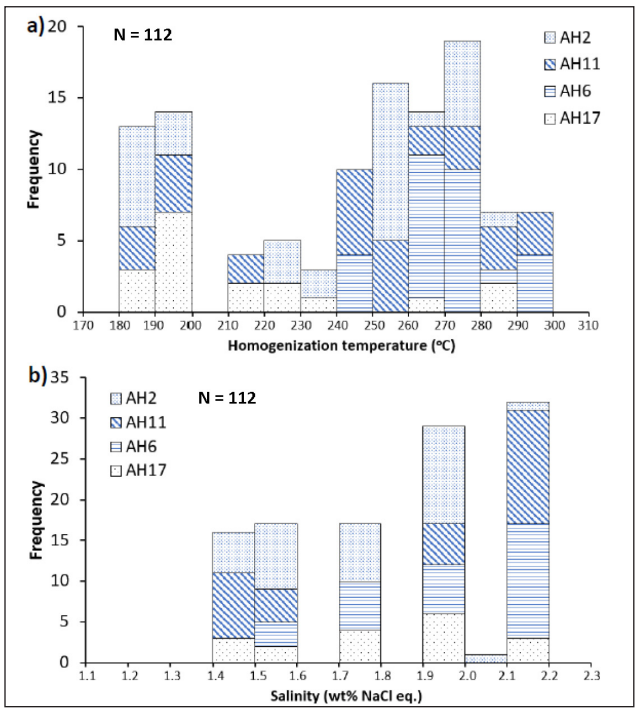

Figure 9: a) Histogram of homogenization temperature (Th), and b) histogram of salinity equivalent to NaCl wt% of fluid inclusions in the quartz veins from the Anggai block.

hydrothermal activity tended to syn- or post-intrusive events as they occurred at the edge of the intrusions (Prihatmoko & Nugroho, 1998). The fine-grained and porphyritic diorites were reported to intercept one of the drilled holes in Anggai (Prihatmoko & Nugroho, 1998). However, an andesite dyke in the Anggai area revealed 7.9 ± 0.2 Ma (Miocene) (Prihatmoko & Nugroho, 1998).

The ore minerals in Anggai include pyrite, chalcopyrite, galena, sphalerite, and gold and silver (Figures 5, 6, & 10). Gold is closely associated with argentite, whereas base metals are rarely found together (Figure 6). The correlation coefficient (r) between Au and Ag, which is 0.459857, also represents this condition (Table 2). However, only Au and Zn have a strong positive correlation, while Au and Cu have a weak positive correlation, and Au and Pb are not correlated (Table 2). On the other hand, the correlation coefficients between Ag and base metals (Cu, Pb, and Zn) are strong positive correlations (Table 2). These conditions suggest two possible metal formations observed in Anggai. Base metals with possibly silver were probably formed first, while gold and silver later formed at a lower temperature, as indicated by the fluid inclusion data. Near the surface, Fe-oxide (i.e., goethite) was present at the latest stage related to the supergene process replacing pyrite along with covellite and chalcocite that occur at the edge of chalcopyrite (Figures 5f & 10).

Micro-thermometry analysis of fluid inclusions reveals a wide range of homogenization temperatures (Th) and salinity. They can be classified into two modes of occurrence, 180-200 °C and 240-280 °C, and 1.4-1.6 and 1.9-2.2 wt% NaCl eq., respectively (Figure 9). During the fieldwork, less information about crosscutting or vein generation was recorded due to more ore excavation by artisanal miners. However, two types of quartz crystals were recognized from fluid inclusion studies, indicating several generations in the quartz vein samples. Prihatmoko & Nugroho (1998) divided quartz veins in the Anggai block into four stages, namely (1) barren quartz vein/veinlets, (2) gold-base metals bearing quartz veins, (3) weakly mineralized calcite veins, and (4) quartz veins/veinlets, associated with calcite (Figure 10). The stage 2 veins is the primary mineralization in the

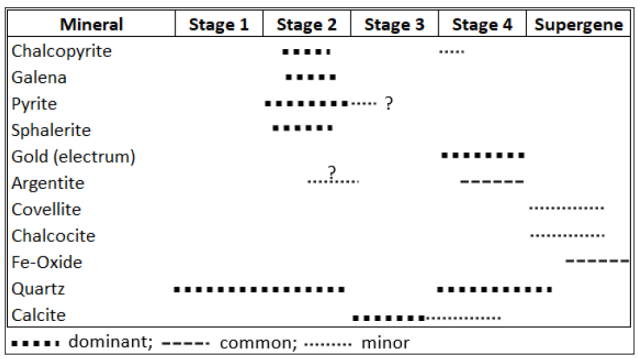

Figure 10: Paragenetic sequence of ore minerals associated with the gold-base metals prospect in Anggai block.

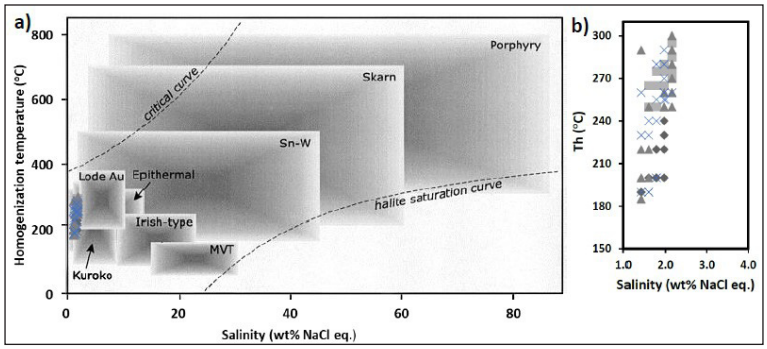

Figure 11: a) Homogenization temperature vs salinity plot of fluid inclusions in the quartz veins from the Anggai block (Modifed from Wilkinson, 2001). b) Exaggerated plot of Figure11a indicating a cooling process of ore-forming fluid and lies on the epithermal type of the gold deposit.

Anggai area that exhibits druzy, comb, colloform banding, and breccia texture in which gold and base metals were found (Prihatmoko & Nugroho, 1998). However, only stage 2 and 4 quartz veins were analyzed for fluid inclusion microthermometry, gaining 250-300 °C and 165-220 °C with 3.2 wt% NaCl eq., respectively (Prihatmoko & Nugroho, 1998). These temperatures are similarly recorded in this study by two modes of occurrences of fluid inclusion (Figure 9). Four samples of fluid inclusion are perhaps derived from these two-stage veins as they show similarity in characteristic and ore mineral assemblages. Two mode occurrences of fluid inclusion suggest the lower temperature is probably related to stage 4 veins that overprinted the stage 2 veins. This condition probably enriched the stage 2 veins with occurrences of gold and base metals in the quartz veins.

Several alteration types were recognized in the Anggai during fieldwork and PIMA analysis, namely argillic and silicic, with limited propylitic alteration. They are zoned from proximal to distal (Nur *et al*., 2016). Alteration mineral assemblages consist of dominant montmorillonite, kaolinite, and silica mineral with minor illite, muscovite, Fe-chlorite, epidote, and carbonate minerals (Figures 8e-f & 10). In addition, adularia was reported in the main alteration zone as a replacement product along with prismatic quartz (Prihatmoko & Nugroho, 1998). These conditions indicate that the ore-forming fluid pH which formed gold and base metals in Anggai was near-neutral to alkaline (Hedenquist *et al*., 1996; Simmons *et al*., 2005). On the other hand, small amounts of dickite, alunite, and halloysite have been recognized so far using PIMA. Those minerals are typical in high-sulfidation epithermal deposits (Hedenquist *et al*., 1996; Simmons *et al*., 2005). Nevertheless, there were no signatures of the occurrence of the acid fluid (i.e., vuggy quartz, alteration type deposit) recognized in the field, becoming more in consideration. According to low temperature, low salinity, and near neutral to alkaline pH, the metals were probably carried by sulfide complex rather than chloride complex (Robb, 2005; Zhu *et al*., 2011; Bodnar *et al*., 2014). In this condition, Cu^{+}, Pb^{2+}, Zn^{2+}, Ag^{+}, and Au^{+} are more stable in hydrothermal solution (Robb, 2005).

The plot diagram of homogenization temperatures (Th) and salinity indicates a cooling of high temperature of the hydrothermal solution (Wilkinson, 2001) (Figure 11). The cooling process is sufficient in the shallower environment as the thermal gradient is higher to a rapid decrease of temperature to promote ore deposition (Wilkinson, 2001; Robb, 2005). Therefore, this condition can be a mechanism to precipitate metals in Anggai. However, Nur *et al*. (2016) concluded that metals were precipitated from a hydrothermal fluid that is isothermally mixed with other contrasted salinity fluids. A slightly decreased salinity as the temperature decreases indicates a greater involvement of meteoric water in the lower temperature or shallower portion in Anggai (Zhu *et al*., 2001) (Figure 10b). This condition is represented by two modes of homogenization temperatures (Th) and salinity of fluid inclusions, indicating an overprinting condition (Wilkinson, 2001) (Figures 9 & 10). In addition, the original ore-forming fluid was probably diluted by oxidized meteoric water in the lower temperature stage to form a small number of sulfate minerals (i.e., alunite and gypsum) in the alteration zone (Robb, 2005).

The low temperature and salinity indicate that mineralization in Anggai was formed in a low sulfidation epithermal system, which is meteoric water in origin. On the other hand, Cu, Pb, and Zn are locally abundant and enriched to form an intermediate-sulfidation deposit at a deeper level (Saunders *et al*., 2014). The Anggai block has recently been at a low elevation of about 50–200 m above sea level. Thus, the host rock and structure intersections have been essential in controlling the gold grade distribution within the quartz vein zone. The gold-base metals in Anggai are primary mineralization driven by the Obi fault, evidenced by the space-filling texture (i.e., banded, laminated, colloform, and crustiform) of quartz veins as ore bodies trending north northwest to south southeast. The Obi fault acted as the conduit to channel the hydrothermal solution to form gold-base metal in Anggai.

CONCLUSIONS

The Obi fault tends to be a conduit to circulate the hydrothermal solution in the Anggai block. The ore bodies are the space-filling texture of quartz veins trending north-northwest to south-southeast. The Oligocene-early Miocene Bacan Formation hosts the gold-base metals prospect, consisting of andesite lavas, volcanic breccia, and tuff. The alteration zones are predominantly argillic in the proximal to limited propylitic to distal, with silicic alteration in specific areas. According to the petrography and geochemical analyses, gold is correlated with argentite, whereas silver is positively correlated with gold and base metals. These conditions suggest two episodes of metal formations in Anggai. Base metals with possibly silver were probably formed first, later formed gold with slightly more silver at the lower temperature. Similarly, homogenization temperatures (Th) and salinity show two modes of occurrences, which are 180-200 °C and 240-280 °C, and 1.4-1.6 and 1.9-2.2 wt% NaCl eq., respectively, suggesting overprinting evidence. This condition probably enriched the ore bodies with occurrences of gold and base metals in the quartz veins. Gold-base metals were probably carried by sulfide complex in the low temperature, low salinity, and near-neutral to alkaline ore-forming fluid. The cooling of hydrothermal solution can be a mechanism to precipitate metals in Anggai. In addition, slightly decreased salinity as the temperature decreased, indicating dilution of ore-forming fluids with more involvement of meteoric water in the lower temperature or shallower portion.

ACKNOWLEDGEMENT

We thank the head and staff of Dinas Pertambangan dan Energi of the North Maluku Province for supporting the fieldwork and providing supplementary information concerning this study. We are also immensely grateful to the Laboratory of Center for Geological Resources (PSDG) of Indonesia for providing valuable discussions during the analyses. Finally, the authors thank the editor-in-chief of this journal for handling this manuscript and the anonymous reviewers for constructive comments and suggestions to make this manuscript eligible to be published.

AUTHOR CONTRIBUTIONS

BNW, MZT, NCDA, and WW are the main contributors. BNW conducted the investigation, and with MZT, NCDA, WW did conceptualization, data analysis, discussion, validation, visualization, roles/writing-original manuscript, writing review, and editing. While HK, IS, BP, AT, and K contributed to validation, writing review, discussion, and editing.

CONFLICT OF INTEREST

There is no conflict of interest to declare.

REFERENCES

Ali, J.R. & Hall, R., 1995. Evolution of the boundary between the Philippine Sea Plate and Australia: Paleomagnetic evidence from eastern Indonesia. Tectonophysics, 251, 251-275. https://doi.org/10.1016/0040-1951(95)00029-1.

Baker, S. & Malaihollo, J., 1996. Dating of Neogene igneous rocks in the Halamahera region: arc initiation and development. In: R. Hall & D. Blundell (Eds.), Tectonic of Southeast Asia. Geological Society Special Publication No. 106.

Bering, D., 1986. The exploration of the Kaputusan copper-gold porphyry (Bacan Island, Northern Moluccas). Federal Institute for Geosciences and Natural Resources, Report 099386, Hannover. 140 p.

Bodnar, R.J., Lecumberri-Sanchez, P., Moncada, D. & Steele-Maclnnis, M., 2014. Fluid inclusions in hydrothermal ore deposits. Treatise on Geochemistry 2nd Edition, Elsevier, 119-141. http://dx.doi.org/10.1016/B978-0-08-095975-7.01105-0.

Clark, L.V. & Gemmell, J.B., 2018. Vein stratigraphy, mineralogy, and metal zonation of the Kencana low-sulfidation epithermal Au-Ag deposit, Gosowong Goldfield, Halmahera Island, Indonesia. Economic Geology, 113, 209-236. http://10.5382/econgeo.2018.4549.

Dow, D.B. & Sukamto, R., 1984. Western Irian Jaya: The end-product of oblique plate convergence in the late Tertiary. Tectonophysics, 106, 109-139. https://doi.org/10.1016/0040-1951(84)90224-5.

Hall, R., Ali, J.R. & Anderson, C.D., 1995. Cenozoic motion of the Philippine Sea Plate: Paleomagmatic evidence from eastern Indonesia. Tectonics, 14(5), 1117-1132. https://doi.org/10.1029/95TC01694.

Hamilton, W., 1979. Tectonics of the Indonesian Region. USGS Prof. Paper 1708, 345 p.

Hedenquist, J.W., Izawa, E., Arribas, A.Jr. & White, N.C., 1996. Epithermal gold deposits: Styles, characteristics and exploration. Resource Geology, Special Publication Number 1.

Malaihollo, J.A. & Hall, R., 1996. The geology and tectonic evolution of the Bacan region, east Indonesia. Geological Society of London Special Publications, 106, 483-497. http://10.1144/GSL.SP.1996.106.01.30.

Nur, I., Irfan, U.R. & La Masinu, A., 2016. Mineralogy and fluid inclusion microthermoetry of epithermal gold-base metal mineralization at Anggai, Obi Island, Indonesia. Sriwijaya International Conference on Engineering, Science and Technology (SICEST), 1-5.

Prihatmoko, S. & Nugroho, F.E., 1998. Tertiary volcanic and intrusive rocks in Obi Islands, Maluku, Indonesia, and related hydrothermal mineralizations. Prosiding Ikatan Ahli Geologi Indonesia, Pertemuan Ilmiah Tahunan XXVII, Yogyakarta.

Robb, L., 2005. Introduction to ore-forming process. Blackwell, United Kingdom. 373 p.

Roedder, E., 1984. Fluid Inclusions. De Gruyter, Berlin, Boston. 644 p.

Saunders, J.A., Hofstra, A.H., Goldfarb, R.J. & Reed, M.H., 2014. Geochemistry of hydrothermal gold deposits. Treatise on Geochemistry 2nd Edition, Elsevier, 383-424. http://dx.doi.org/10.1016/B978-0-08-095975-7.01117-7

Simmons, S.F., White, N.C. & John, D.A., 2005. Geological characteristics of epithermal precious and base metal deposits. In: Jeffrey W. Hedenquist, John F.H. Thompson, Richard J.

Goldfarb & Jeremy P. Richards (Eds.), Society of Economic Geologist 100th Anniversary Volume, 485-522. https://doi.org/10.5382/AV100.16.

Sudana, A., Yasin & Sutisna K., 1994. Geological Map of the Obi Sheet, Maluku, Scale of 1: 250,000. Geological Research and Development Centre, Bandung.

Sudarya, S. & Faisal, R., 2007. Inventarisasi Mineral Logam di Kabupaten Halmahera Selatan dan Kota Tidore Kepulauan, Provinsi Maluku Utara. Bandung. Proceeding Pemaparan Hasil Kegiatan Lapangan dan Non-lapangan Tahun 2007 Pusat Sumber Daya Geologi. 9 p.

van Leeuwen, T., 2018. Twenty five more years of mineral exploration and discovery in Indonesia (1993-2017). Masyarakat Geologi Ekonomi Indonesia 10th Anniversary Special Publication, 318 p.

Wilkinson, J.J., 2001. Fluid inclusions in hydrothermal ore deposits. Lithos, 55, 229-272. https://doi.org/10.1016/S0024-4937(00)00047-5.

Zhu, Y., An, F. & Tan, J., 2011. Geochemistry of hydrothermal gold deposits: A review. Geoscience Frontiers, 2(3), 367-374. https://doi.org/10.1016/j.gsf.2011.05.006.

Zhu, Y., Jiang, N. & Zeng, Y.S., 2001. Geochemistry of ore-forming fluids in gold deposits from the Taihang Mountains, Northern China. International Geology Review, 43, 457-473. http://10.1080/00206810109465026.

Manuscript received 15 August 2023;
Received in revised form 20 October 2023;
Accepted 26 October 2023
Available online 30 May 2024